Free-Electron Computed Tomography of Near-Fields

Tamir Shpiro, Ron Ruimy, Tomer Bucher, Avner Shultzman, and Ido Kaminer
Andrea & Erna Viterbi Department of Electrical and Computer Engineering, Technion–Israel Institute of Technology, 3200003 Haifa, Israel.
kaminer@technion.ac.il

Abstract: We propose a novel approach for extracting the 3D vectorial near-field confined in nanostructures. Our Radon-like algorithm incorporates the nonlinearity of free-electron interactions and can be realized using ultrafast transmission electron microscopes.

Studies of electromagnetic near-field dynamics in nanostructures stand at the core of light-matter interactions, with important applications in nanophotonics [1]. Various approaches have been developed to achieve spatio-temporal imaging of near-fields with high resolution in space and time. The two most prolific approaches used for this purpose are Photo-Emission Electron Microscopy (PEEM) [2] and scattering-type Scanning Near-field Optical Microscopy (sSNOM) [3], both extracting the near-fields along *surfaces*. A more recent, swiftly evolving method, Photon-Induced Near-field Electron Microscopy (PINEM) [4], has the potential to image near-fields *inside* nanostructures [5]. PINEM relies on inelastic scattering between electrons and illuminated nanostructures (Fig. 1b$_1$) in transmission electron microscopy (TEM). Established TEM techniques use sequences of images at varying rotations for 3D tomographic reconstructions of various materials and phenomena, from inner structures of biological specimens [6] and magnetic field distributions in magnetic structures [7] to local density of photonic states within nanophotonic structures [8].

Despite this substantial recent progress, 3D tomographic reconstruction of *electromagnetic near-fields* has remained beyond reach. The goal of near-field tomography is particularly intriguing considering the fast-paced growth of nanoscale 3D printing technologies and other nanofabrication processes [9], which create nanostructures with intricate electromagnetic responses, from metasurfaces and 2D materials to silicon photonic waveguides and integrated frequency combs. The ability to image the complex vectorial near-fields in-situ, i.e., *inside* such structures, could be of great value for frontier challenges in these fields, especially when involving their optical nonlinear responses. However, these prospects have remained unexplored. Conventional tomographic schemes cannot be applied for time-harmonic fields, such as the near-field in nanophotonics.

Here we present a novel approach for 3D reconstruction of time-harmonic near-fields, accounting for their complex-valued vectorial nature. We propose a concrete implementation for illuminated nanostructures in ultrafast TEMs, denoted as Free-Electron Computed Tomography (FECT). We develop a Computed Tomography (CT) [10] algorithm tailored for time-harmonic complex vector fields, relying on the PINEM interaction (Fig. 1a). FECT necessitates acquiring both *amplitude and phase* of the near-field projected along the measurement angles. This capability was recently achieved using modulated free electrons [11-13] (Fig. 1b$_2$), making the implementation of FECT feasible in existing experimental platforms (Fig. 1b$_3$).

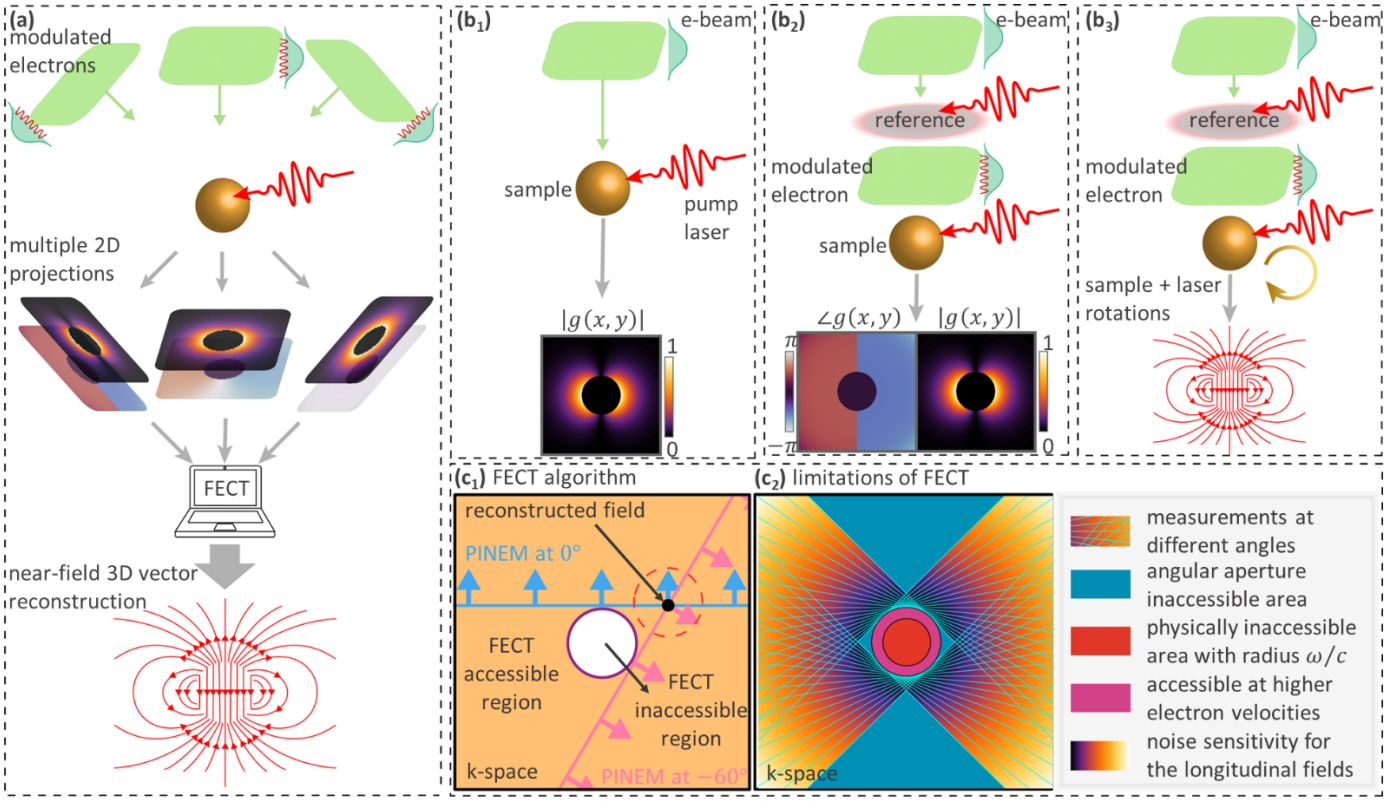

Fig.1 Free-electron computed tomography (FECT): concept, implementation, and algorithm. (a) FECT concept. **(b)** Proposed implementation, comparing standard PINEM (b$_1$), complex-field reconstruction (b$_2$), and our tomographic scheme (b$_3$). **(c)** The FECT algorithm, explaining the basic principle and limitations. Accessible k-space regime (outside a circle with radius ω/v) and example point for which the full vectorial electric field is reconstructed from crossing two complex-field PINEM measurements (c$_1$). FECT limitations, showing the accessible and inaccessible regions, overlaid by noise sensitivity in the longitudinal field (c$_2$).

The theory of FECT relies on the same interaction as in PINEM, between free electrons (velocity v in the $-\hat{z}$ direction) and optical near-fields, approximated as time-harmonic $\vec{E}(x,y,z)\cdot e^{i\omega t}$. The interaction strength follows the dimensionless parameter:

$$g(x,y)=\frac{e}{\hbar\omega}\int_{-\infty}^{\infty}\hat{z}\cdot\vec{E}(x,y,z)e^{-iz\omega/v}\,dz. \quad (1)$$

Pre-modulation of the electrons enables extracting both the phase and amplitude of g at every point x,y (Fig. 1b$_2$) [11-13]. The resulting $g(x,y)$ is the Fourier component of the scalar function $\hat{z}\cdot\vec{E}(x,y,z)$ with respect to the variable z at wavevector $k_z=$

ω/v. Fourier transforming the xy axes yields a 2D map of Fourier components k_x, k_y for this fixed $k_z = \omega/v$. By tilting the interaction axis and repeating this process, we retrieve a sequence of complex 2D Fourier maps, each representing a different planar k-space cross-section along a plane shifted from the origin by a wavevector of size ω/v and direction of the electron motion relative to the sample. Such projections are "frequency-shifted" by $k_z = \omega/v$, contrary to the situation in all other approaches of tomography. Conventional projections, as in X-ray CT, could only be achieved when $v \to \infty$, which is irrelevant for imaging optical fields since their intrinsic velocity is larger than that of the imaging particle.

We develop an algorithm for the reconstruction of the 3D complex vector field, using a modified Radon-type transform, adjusted for both the frequency-shifted projection and the vector-field nature. PINEM poses a certain limit on the reconstruction: k-space components inside a sphere of radius ω/v cannot be retrieved (Fig. 1c$_1$). This limitation is fundamental since electrons only interact with frequencies higher than ω/v, as illustrated by the Lawson-Woodward theorem [14]. Our example in Fig. 2 shows that this limitation does not necessarily hamper the reconstruction of desired confined near-fields in nanophotonics.

Our FECT algorithm implements back-projection for PINEM measurements taken for a finite number of angles over a certain pre-set range (Fig. 1b). The algorithm crosses three planes through each accessible point in k-space. Each plane supplies another field component (normal to the plane). This way, three different planes provide sufficient information for the complete reconstruction of the vectorial components at a point in k-space (Fig. 1c$_1$). To execute FECT, we propose the following procedure: each PINEM measurement using modulated electrons provides a highly nonlinear measurement, from which the complex-valued $g(x,y)$ can be reconstructed [11]. After applying this process on enough angles, FECT back-projects the field. This procedure can be described as a linear operator acting on the electric field, having a non-trivial null-space containing all the frequencies lower than ω/v. Reconstruction of additional information beyond the confined near-field requires additional assumptions about the field.

Further technical constraints of FECT are high-frequency noise sensitivity and the incomplete range of angles accessible by the TEM (Fig. 1c$_2$). We can address these challenges by adopting a wide range of established approaches from conventional optical tomography [15]. The type of noise sensitivity we experience in FECT is intriguing, as it arises from having a combination of a vector field and a frequency shift. High-momentum points in k-space (with respect to ω/v) are extremely sensitive to noise (Fig. 1c$_2$), because at these points, normal vectors to planes tangential to the sphere have a very small component in the radial direction. Imposing physical assumptions about the field, such as using Maxwell's equations, could serve to reduce the noise. Alternatively, more information can be provided by measuring with several v values to modify the radius of the sphere in k-space.

To exemplify FECT, we apply it to simulated measurements of an illuminated gold nano-wire that is long enough to be described by an effectively 2D field. To collect the projections, we rotate the nanowire around its axis perpendicular to the electron path. Figs. 2b$_2$, 2c$_2$ and 2d$_2$ show the similarity between the scattered electric field, the confined electric field (meaning, only frequencies higher than ω/c), and the electron-accessible field (same with ω/v). Fig. 2e shows the improvement of the reconstruction for better TEM resolution and for more measurements. Good results can be seen already with just 7 measured angles. The error approaches zero for infinitesimal resolution. To mitigate the high discretization errors caused by sensitivity to high-frequency noise, we apply a Gaussian filter to the reconstructed image.

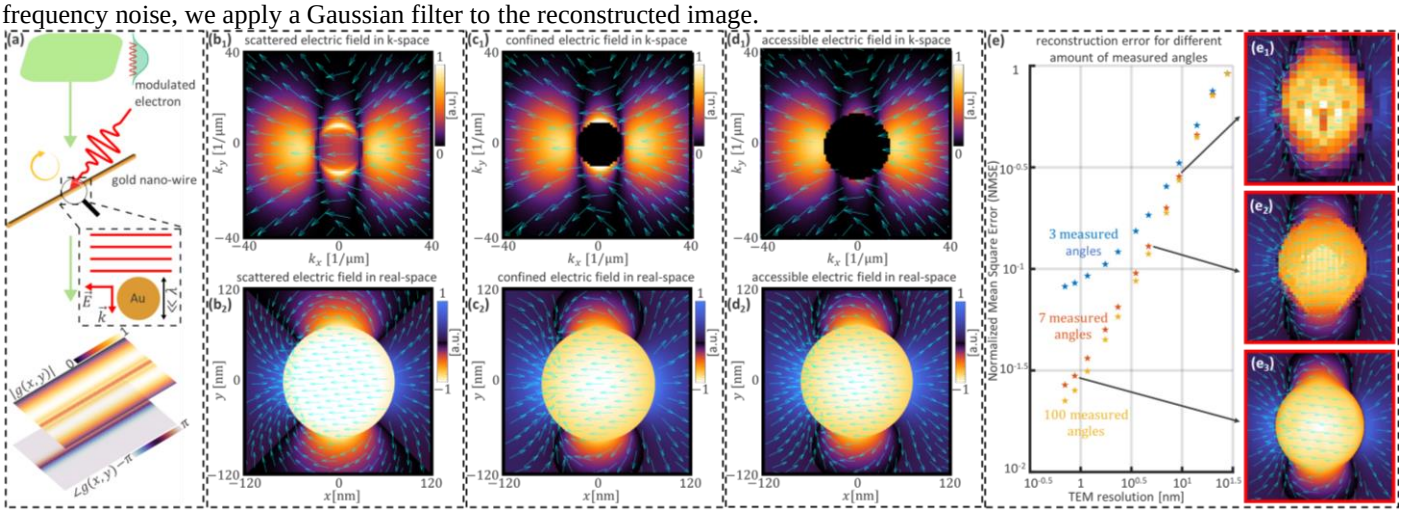

Fig.2 The concept of FECT simulated for a nanowire. (a) PINEM measurements of a long gold nano-wire excited by a planewave (polarization and k-vector both perpendicular to the wire axis). The long dimension of the wire makes this configuration effectively 2D. **(b)** The scattered electric field in k-space and real-space. **(c)** The confined electric field in k-space and real space (effectively, a high-pass-ω/c-filtered field). **(d)** The electric field that can interact with the electron in k-space and real space (effectively, a high-pass-ω/v-filtered field). **(e)** Normalized Mean Square Error (NMSE) value of the reconstruction as a function of the TEM resolution, converging to perfect reconstruction for a different number of measured angles (different colors). Both axes are log scaled. **Note that the vectorial nature of the field is accurately reconstructed, even in areas where the reconstructed field amplitude is not accurate**. All panels assume 200 keV electrons, a 140 nm diameter gold nano-wire, and a 700 nm laser illumination.

Future research can rely on our approach to reconstruct the complete scattered field for various 3D nanostructure, within the confines of physical, experimental, and computational limitations. Future improvements can rely on physical principles directly from Maxwell's equations, on the use of tomographic sparse representation methods [16], and on iterative reconstruction algorithms.

[1] L. Novotny and B. Hecht, *Principles of Nano-Optics* (Cambridge University Press, 2012).
[2] S. Nelayah, et al., *Nat. Phys.* **3**, 348–353 (2007).
[3] S. Tesses, et al., *Science.* **361**, 6406 (2018).
[4] B. Barwick, et al., *Nature.* **462**, 902–906 (2009).
[5] T. Lummen, et al., *Nat. Commun*. **7**, 13156 (2016).
[6] J. Frank, *Electron Tomography*. (Springer, 2006).
[7] D. Wolf, et al., *Commun. Phys.* **2**, 87 (2019).
[8] A. Hörl, et al., *Nat. Commun.* **8**, 37 (2017).
[9] H. Y. Jeong, et al., *Nanophotonics.* **9**, 5 (2020).
[10] T. Buzug, *Computed Tomography: From Photon Statistics to Modern Cone Beam CT* (Springer, 2008).
[11] T. Bucher, et al., arXiv:2305.02727 (2023).
[12] J. H. Gaida, et al., arXiv:2305.03005 (2023).
[13] D. Nabben, et al., *Nature*. **619**, 63-67 (2023).
[14] J. D. Lawson, *IEEE Trans. Nucl. Sci.* **26**, 4217 (1979).
[15] J.W. Lim, et al., *Opt. Express.* **23**, 13 (2015).
[16] M. Elad, *Sparse and Redundant Representations: From Theory to Applications in Signal and Image Processing* (Springer, 2010).